Dissolved Gases in Seawater

- Fundamentals
- Solubility Relationships
- Air-Sea Exchange
- Departures from Ideality
- O_2 Dynamics (Intro)

DISSOLVED GASES IN THE OCEANS

SOURCES

1. Atmosphere (Major Term)
   (N_2, O_2, Ar, etc.)

2. Volcanic Activity (H_2S)

3. Marine Production & Consumption Proce

   a) Biological Activity
      ($NO_3^- \rightarrow N_2O$, respiration)
   b) Radioactive Decay
      ($^{226}Ra \rightarrow {}^{222}Rn$)

BASIC CONCEPTS

I. Dalton's Law

$$P_T = \Sigma P_i \sim P_{N^2} + P_{O^2} + P_{Ar} + P_{H^2O} + P_{CO2}$$

II. Ideal Gas Law

$$P_i = n_i RT/V \text{ where } R = 82.05 \text{ cm}^3 \text{ atm mol}^{-1}\text{deg}^{-1}$$

III. $P_i = X_i [P_T - P_{H^2O}]$, $P_{H^2O} = (h/100)\, P_{H^2O\text{-Sat}}$

IV. Henry's Law

$$C_i = K_i [P_i] \qquad P_i \sim f_i$$

at equilibrium P_i (soln) = P_i (air)

$$K_i = f(T,S,P)$$

Dissolved Gases in Seawater

- Fundamentals
- Solubility Relationships
- Air-Sea Exchange
- Departures from Ideality
- O_2 Dynamics (Intro)

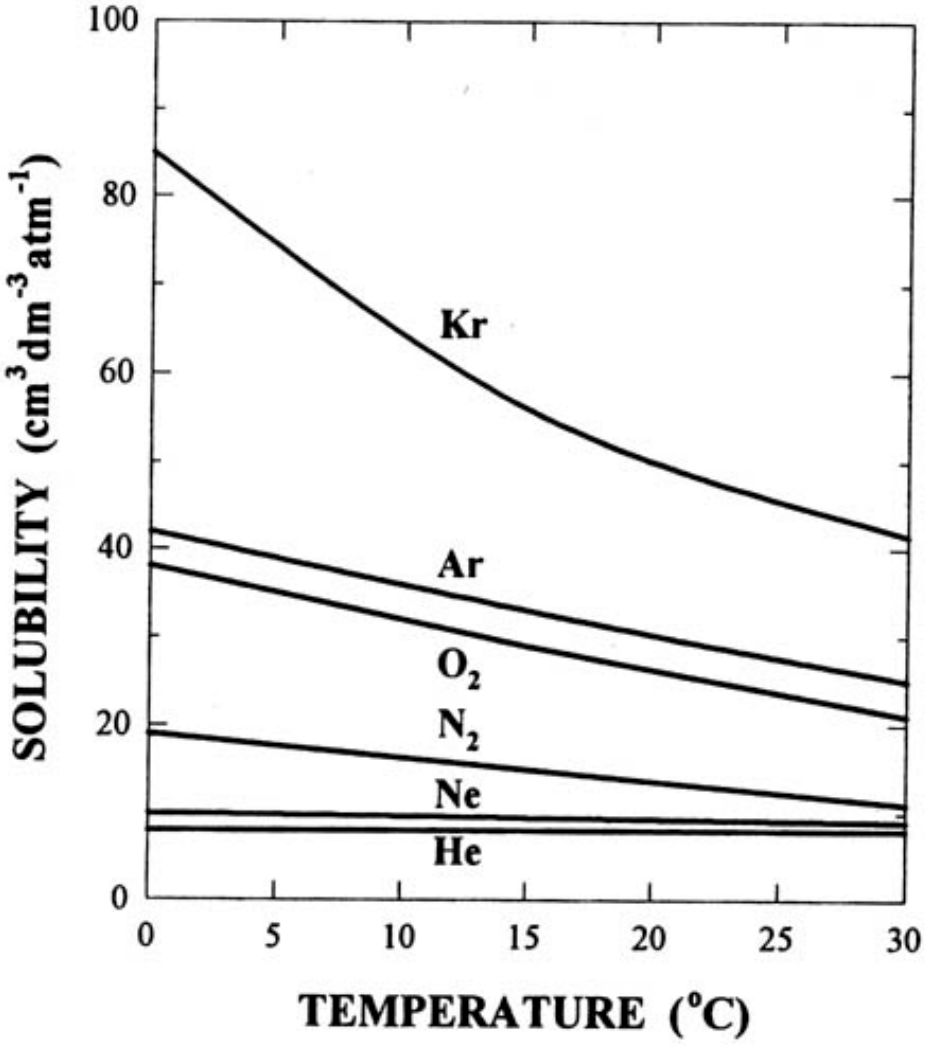

FIGURE 6.5. The effect of temperature on the solubility of gases in seawater.

Table 3.6. *Solubilities of the major atmospheric gases in seawater (s = 35) at one atmosphere pressure and 20 °C*

X_C is the mole fraction in a dry atmosphere (Glueckauf, 1951); $K_{H,C}$, the Henry's Law coefficient; C^s, the concentration in seawater at saturation equilibrium with the atmosphere. Saturation concentrations and Henry's Law coefficients for N_2, O_2, Ar, CO_2, Ne and He are calculated by using the equations in Table 3A1.1. Values for Kr, CH_4 and N_2O are from the compilation in Wanninkhof (1992). No correction was made here for the difference between the volume of the solvent and the solution in β and α (see text).

Gas	X_C	$K_{H,C}$	C^{sa}	β^b	α^c
	$(mol_g\ mol_{atm}^{-1})$	$(mol\ kg^{-1}atm^{-1})$	$(\mu mol\ kg^{-1})$	$(cm_g^3)/(cm_{sw}^{-3})$	
N_2	7.8084×10^{-1}	5.51×10^{-4}	4.21×10^{2}	1.27×10^{-2}	1.36×10^{-2}
O_2	2.0946×10^{-1}	1.10×10^{-3}	2.25×10^{2}	2.53×10^{-2}	2.71×10^{-2}
Ar	9.34×10^{-3}	1.21×10^{-3}	1.10×10^{1}	2.78×10^{-2}	2.98×10^{-2}
CO_2	3.65×10^{-4}	3.24×10^{-2}	1.16×10^{1}	7.44×10^{-1}	7.98×10^{-1}
Ne	1.818×10^{-5}	3.84×10^{-4}	6.83×10^{-3}	8.82×10^{-3}	9.47×10^{-3}
He	5.24×10^{-6}	3.29×10^{-4}	1.66×10^{-3}	7.47×10^{-3}	8.01×10^{-3}
Kr	1.14×10^{-6}	2.20×10^{-3}	2.44×10^{-3}	5.05×10^{-2}	5.42×10^{-2}
CH_4	1.6×10^{-6}	1.21×10^{-3}	1.89×10^{-3}	2.78×10^{-2}	2.97×10^{-2}
N_2O	5.0×10^{-7}	2.34×10^{-2}	1.14×10^{-2}	5.37×10^{-1}	5.77×10^{-1}

EFFECT OF TEMPERATURE ON SOLUBILITY OF GASES IN SEAWATER

Gas	0°C	25°C
He	1.8 nM	1.7 nM
Ne	7.9	6.6
Kr	4.0	2.3
Xe	0.6	0.4
N_2	616 µM	383 µM
O_2	349	206
Ar	17	10
N_2O	14	6
CO_2	20	9

EFFECT OF SALINITY ON SOLUBILITY OF GASES (0° C)

Gas	Water	Seawater
He	2.2 nM	1.8 nM
Ne	10	7.9
Kr	5.8	4.0
Xe	0.9	0.2
N_2	823 µM	616 µM
O_2	456	349
Ar	22	17
CO_2	23	20

Table 3A1.1. *Coefficients used in the fitting equations for air saturation (C^s) and Henry's Law coefficients (K_H) of gases in seawater (Table 3.6)*

The coefficients and fitting equations in the footnotes are for saturation values of O_2, N_2, Ar, Ne, and He in units of μmol kg^{-1} and ml kg^{-1}. Values can be transformed between these units by using the real gas molar volumes calculated from Van der Waals constants (22.385 9, 22.391 9, 22.386 9, 22.422 4 and 22.436 9 mol^{-1} for O_2, N_2, Ar, Ne, and He, respectively). The fitting equation for CO_2 is for the Henry's Law coefficient, K_H (mol kg^{-1} atm^{-1}) instead of the saturation concentration.

	O_2[a]	N_2[b]	Ar[b]	Ne[b]	He[c]	K_{H,CO_2}[d]
Coefficient		(μmol kg^{-1})		(nmol kg^{-1})	(ml kg^{-1})	(mol kg^{-1}atm^{-1})
A_0	5.808 710	6.432 41	2.791 63	2.181 40		
A_1	3.202 910	2.927 58	3.177 14	1.289 31	−67.217 8	−60.240 9
A_2	4.178 870	4.303 51	4.136 58	2.122 35	216.344 2	93.451 7
A_3	5.100 060	4.266 73	4.866 32		139.203 2	23.358 5
A_4	−0.098 664				−22.620 2	
A_5	3.803 690					
B_0	−0.007 016	−0.007 443 16	−0.006 963 17	−0.005 947 22		
B_1	−0.007 700	−0.007 999 36	−0.007 683 87	−0.005 093 70	−0.044 781	0.023 517
B_2	−0.013 86	−0.001 529 48	−0.001 190 78		0.023 541	−0.023 656
B_3	−0.009 515				−0.0034266	0.0047035
C_0	$-2.759\,150 \times 10^{-7}$					
$[C]^s$ at 20 °C 35 ppt	225.5	420.5	11.08	6.826	3.729×10^{-5}	0.0324

[a] Garcia and Gordon (1992): $\ln C^s = A_0 + A_1T_s + A_2T_s^2 + A_3T_s^3 + A_4T_s^4 + A_5T_s^5 + S(B_0 + B_1T_s + B_2T_s^2 + B_3T_s^3) + C_0S^2$;
where $T_s = \ln\{(298.15 - t)(273.15 + t)^{-1}\}$ and t is temperature (°C).

[b] Hamme and Emerson (2004): same equation as in [a].

[c] Weiss (1971): $\ln C^s = A_1 + A_2(100/T) + A_3\ln(T/100) + A_4(T/100) + S\{B_1 + B_2(T/100) + B_3(T/100)^2\}$, where T is absolute temperature.

[d] Weiss (1974): $\ln K_{H,CO_2} = A_1 + A_2(100/T) + A_3\ln(T/100) + S\{B_1 + B_2(T/100) + B_3(T/100)^2\}$, where T is absolute temperature.

Dissolved Gases in Seawater

- Fundamentals
- Solubility Relationships
- Air-Sea Exchange
- Departures from Ideality
- O_2 Dynamics (Intro)

Fick's First Law

$$dC_i/dt = A\, D_i\, (dC_i/dz)$$

Where:

A = area

C_i = concentration species i

D_i = diffusion coefficient

Z = thickness of diffusion layer

Table 10.1. *Molecular diffusion coefficients, D, and Schmidt numbers, Sc, for gases*

The molecular diffusion coefficients, D (in units of 10^{-5} cm^2 s^{-1}; see note[a]), were determined from the equations presented in Chapter 9, Table 9.1. The kinematic viscosity of water is from Pilson (1998). The kinematic viscosity is 3%–5% greater in seawater than in freshwater, and we assume here that this is the only factor causing a salinity dependence on Sc. Opposite trends with T for diffusion coefficients and kinematic viscosity create greater temperature dependence for Schmidt numbers than for the molecular diffusion coefficients.

	D ($\times 10^5$)[a] (cm^2 s^{-1})		Sc[b] ($S=0$)		Sc[c] ($S=35$)	
Gas	5 °C	20 °C	5 °C	20 °C	5 °C	20 °C
N_2	1.63	2.52	931	398	958	415
O_2	1.49	2.24	1019	448	1048	467
Ar	1.42	2.23	1070	450	1100	469
CO_2	1.09	1.68	1394	598	1433	623
Ne	2.62	3.65	580	275	596	287
He	5.19	6.73	293	149	310	155
Kr	1.03	1.61	1475	624	1516	650
Xe	0.79	1.27	1923	791	1977	823
CH_4	1.09	1.63	1394	616	1433	642

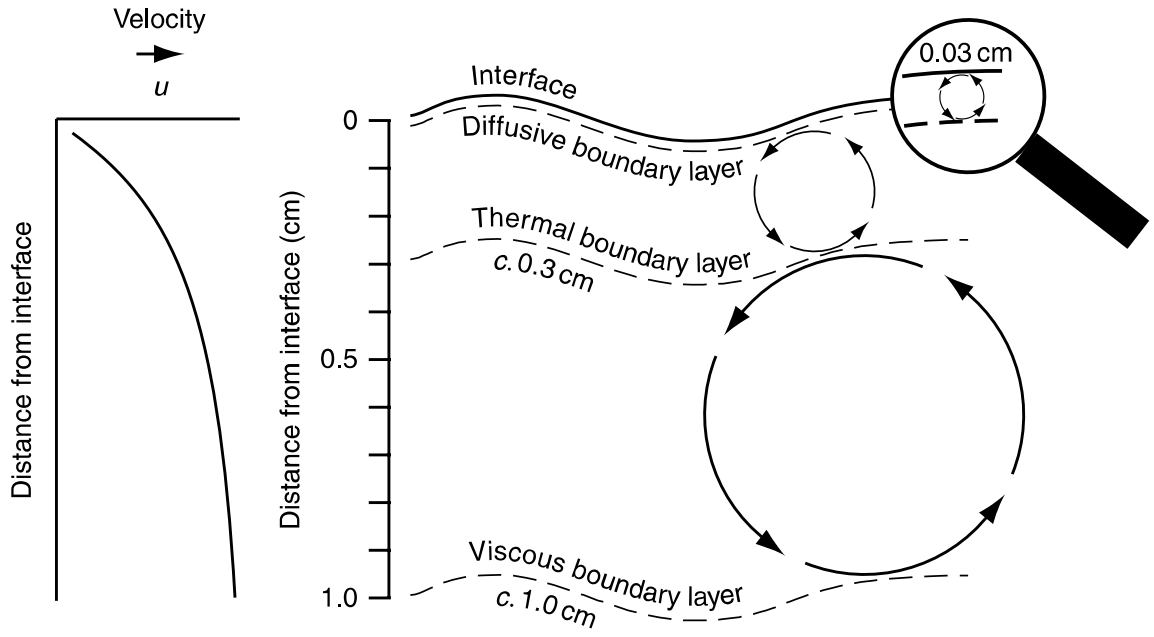

Figure 10.1. A schematic representation of the boundary layers for momentum, heat and mass near the air–water interface. The velocity of the water and the size of eddies in the water decrease as the air–water interface is approached. The larger eddies have greater velocity, which is indicated here by the length of the arrow in the eddy. Because random molecular motions of momentum, heat and mass are characterized by molecular diffusion coefficients of different magnitude (0.01 $cm^2 s^{-1}$ for momentum, 0.001 $cm^2 s^{-1}$ for heat and 10^{-5} $cm^2 s^{-1}$ for mass), there are three different distances from the wall where molecular motions become as important as eddy motions for transport. The scales are called the viscous (momentum), thermal (heat) and diffusive (molecular) boundary layers near the interface.

Models for Air-Sea Gas Exchange

1) Stagnant Film (simplest)

2) Surface Renewal

3) Rigid Wall (Mathematically complex)

Figure 10.2. A schematic diagram of the stagnant molecular layers near the air–water interface. Fugacity in the bulk atmosphere and concentration in the water are indicated by f^a and [C], respectively. Chemical equilibrium at the air–water interface is described by Henry's Law, where $K_H f^a_{sat} = [C^{Sat}]$.

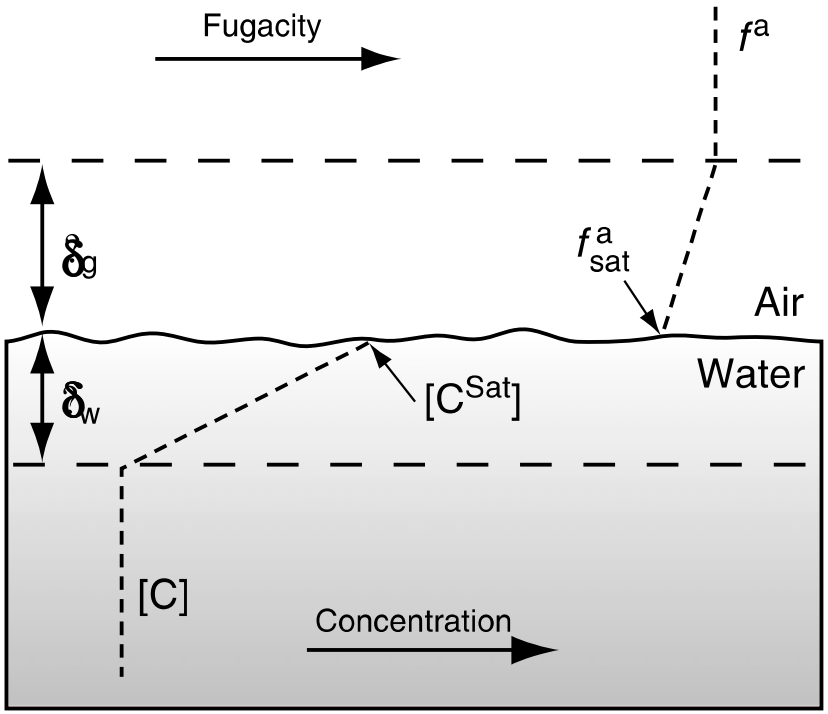

Combining Henry's and Fick's Laws:

$$dC_i/dt = (A\ D_i\ H_i\ /\delta\ )\ [P_i\ (gas)\ -\ (P_i\ (liquid)]$$

where:

τ = **thickness of boundary layer**

More simply:

$$F_i = dC_i/dt = G_c K_i \Delta P_i$$

$$G_c = G^* (D_i/\nu)^n = G^* (Sc_i)^{-n}$$

Where:

F = flux (mol cm^{-2} s^{-1})

ΔP_i = change in partial pressure across interface (mol cm^{-3})

Sc_i = Schmidt number

ν =kinematic velocity

G^* = transfer velocity (cm s^{-1})

= permeability coefficient

= mass transfer coefficient

= exit coefficient

= piston velocity

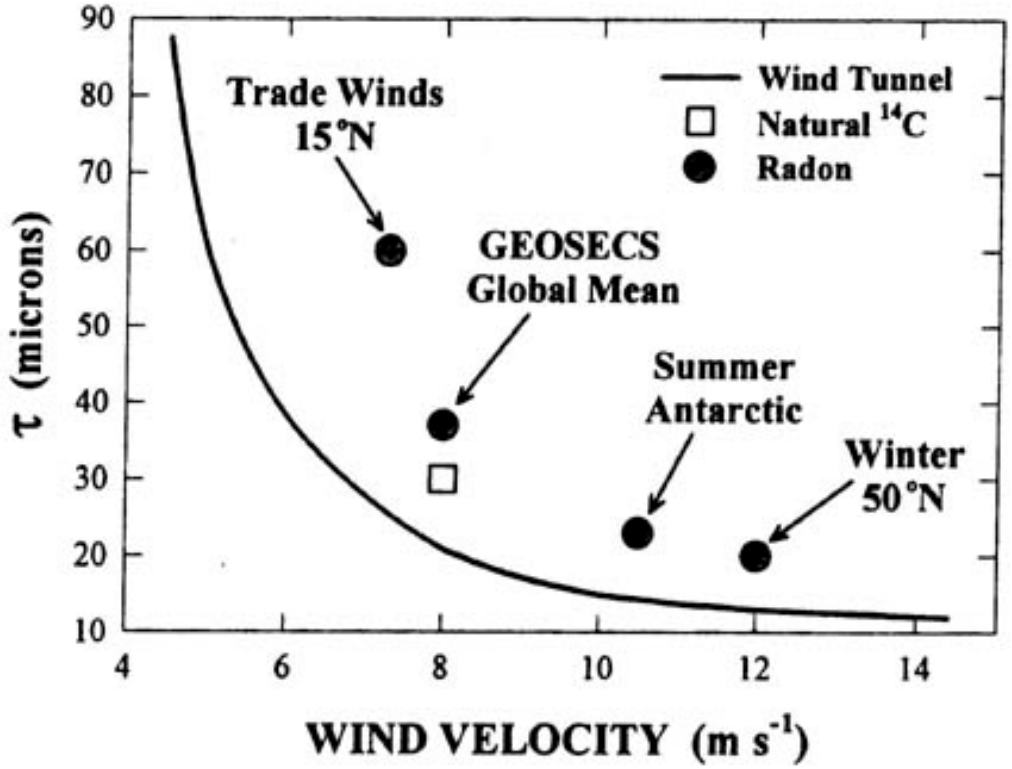

FIGURE 6.2. The thickness of the laminar layer as a function of the wind speed.

Models for Air-Sea Gas Exchange

1) Stagnant Film $G_c = D_i/\delta$

2) Surface Renewal $G_c = 2 (D_i/\pi \theta)^{0.5}$

θ **is renewal time**

3) Rigid Wall $G_c = U^* /12 \ (D_i/\nu)^{2/3}$

$= U^* /12 \ (Sc_i)^{-2/3}$

U* is the friction velocit at the interface

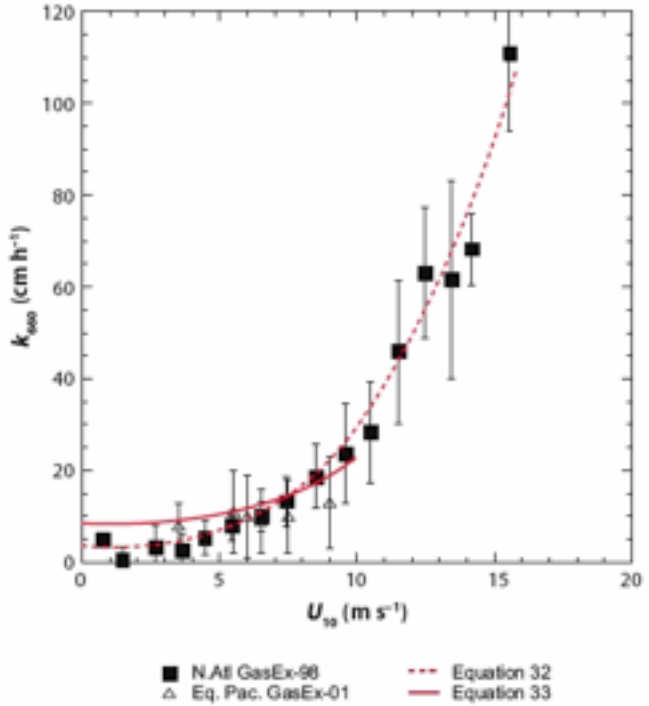

Figure 4

Comparison of CO_2 covariance flux measurements in the North Atlantic (*solid squares*) (McGillis et al.
and Equatorial Pacific (*open triangles*) (McGillis et al. 2004b, Hare et al. 2004). The results are binned i
nominally 1 m s^{-1} wind speed bins and the error bars indicate the standard deviation of the points in e
interval that range from as few as 4 at low and high winds to more than 200 at intermediate winds. The
dashed red line is the parameterization expressed in Equation 32 and the solid red line is that in Equati

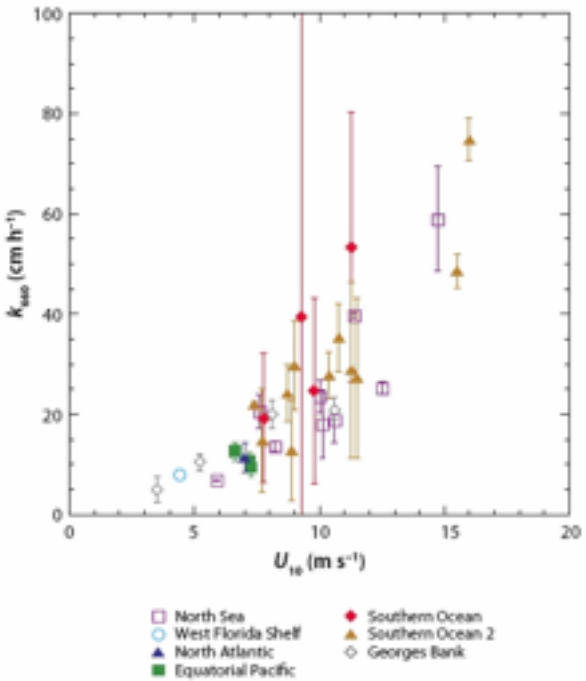

Figure 3

Summary of ^{3}He/SF$_6$ dual-deliberate tracer results normalized to Sc = 660 and plotted against wind speed. The open symbols are for the experiments in the coastal oceans, while the solid symbols depict the studies in the open ocean. The error bars are based on the variation of ^{3}He/SF$_6$ in the mixed layer at each sampling time propagated through Equation 18. References are as follows: North Sea, Nightingale et al. (2000b); West Florida Shelf, Wanninkhof et al. (1997); North Atlantic, Wanninkhof & McGillis (1999); Equatorial Pacific, Nightingale et al. (2000a); Southern Ocean, Wanninkhof et al. (2004); Southern Ocean 2, Ho et al. (2006); Georges Bank, Wanninkhof et al. (1993).

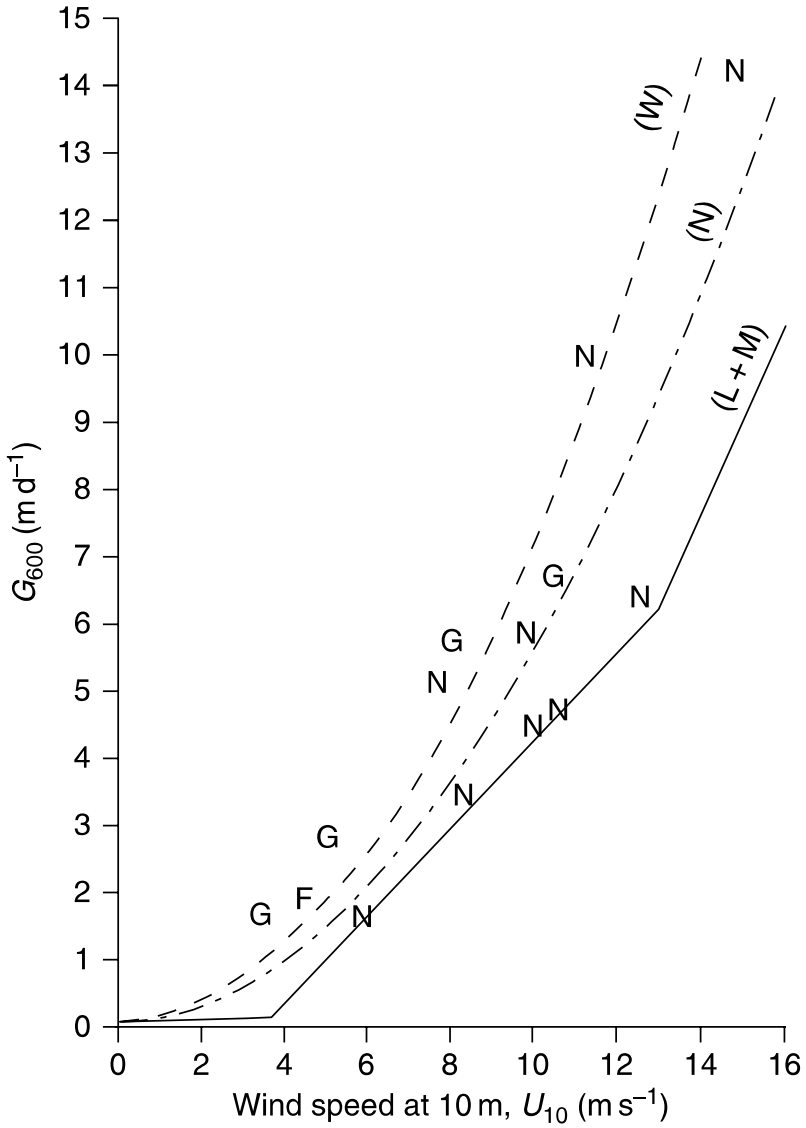

Figure 10.7. Gas transfer velocity, G_{600}, as a function of wind speed, U_{10}, for all dual tracer experiments. N is from the North Sea, G is from the Georges Bank and F from the Florida Shelf. Lines are the same as those described in the caption to Figure 10.6, with the addition of the one in the middle, which is the best fit through the dual tracer data ($G_{600} = \{0.23 \times U^2 + 0.1 \times U\}$ $(Sc/600)^{-1/2}$, where U is in m s^{-1} and G is in cm h^{-1}). Redrawn from Nightingale *et al.* (2000).

Dissolved Gases in Seawater

- Fundamentals
- Solubility Relationships
- Air-Sea Exchange
- Departures from Ideality
- O_2 Dynamics (Intro)

Figure 10.8. Measured oxygen concentrations in ocean surface waters as a function of temperature from the WOCE data base. The line marks the saturation value with atmospheric oxygen at a salinity of 35.

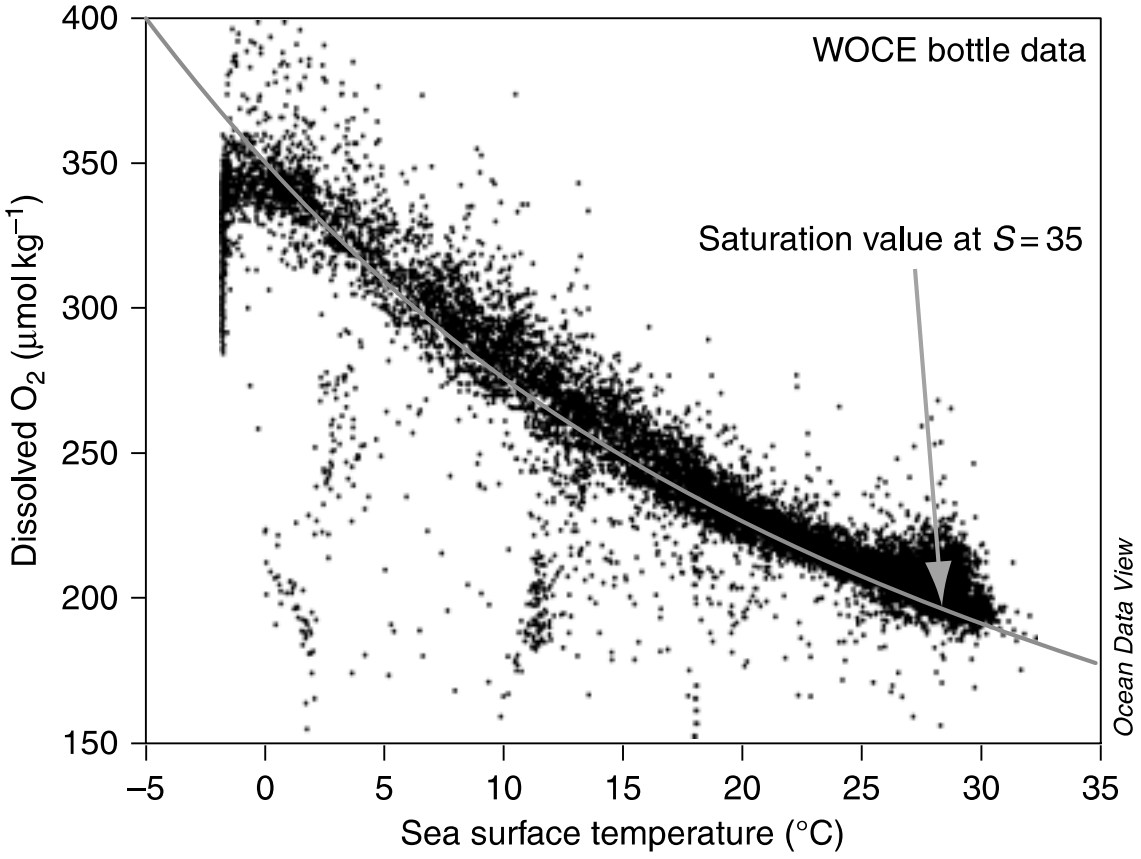

Causes of Non-Reactive Gases Departing from Expected Solub

1. Departures from Standard Atmosphere
2. Dissolution of Air Bubbles
3. Air Injection
4. Differential Heating and Gas Exchange
5. Mixing of Waters of Different Temperatures
6. Radiogenic or Primordial Addition

Figure 10.10. A schematic diagram illustrating two mechanisms of bubble-induced gas exchange. Air injection (total trapping) indicated by the empirical constant V_{inj} is indicated by smaller bubbles that collapse totally as they are subducted into the water by a wave. Exchange (partial trapping) indicated by the empirical constant V_{ex} is for larger bubbles that are submerged by waves and exchange their contents partly with the surrounding water before they resurface at the interface.

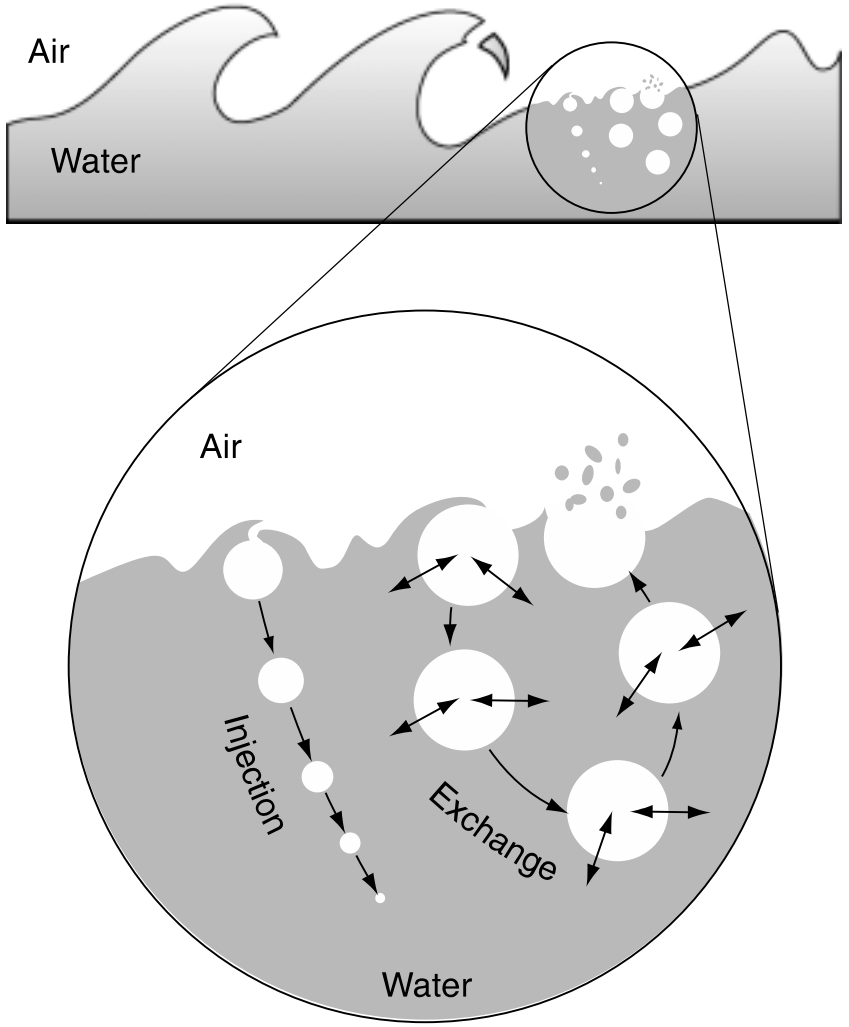

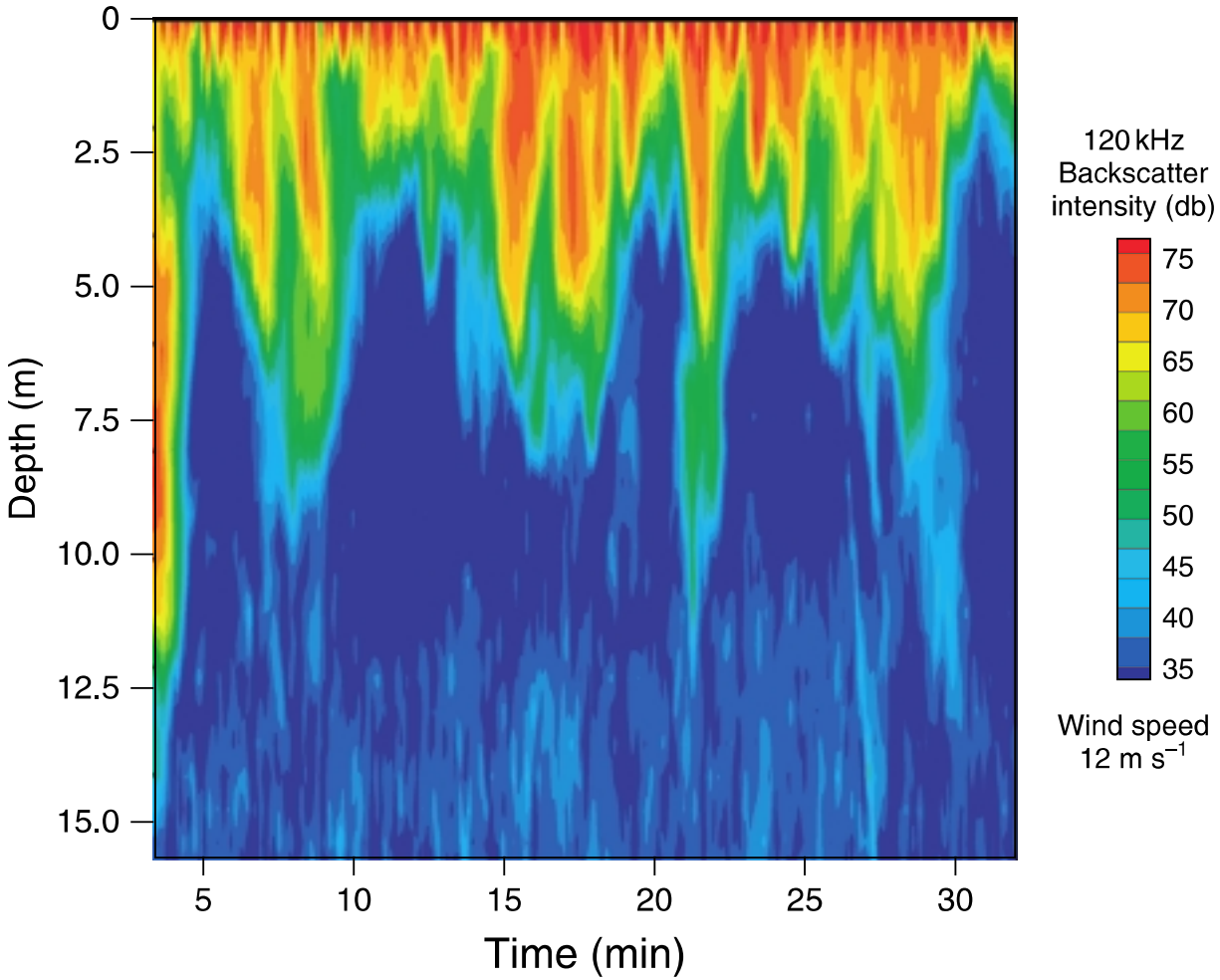

Plate 7 The intensity of acoustic back scatter as a function of depth in the ocean at Stn. P in the subarctic Pacific at a wind speed of 12 m s^{-1}. Back scatter intensity is an indication of the depth of penetration of bubbles caused by breaking waves. (Data courtesy of Sven Vegel of the Institute of Ocean Sciences, Sidney, B. C.).

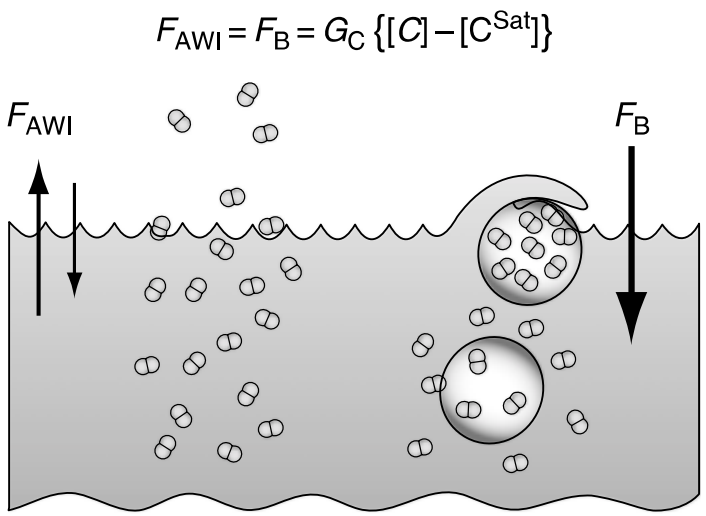

Figure 10.11. A schematic diagram of steady-state gas supersaturation caused by bubble processes when there is no net flux at the air–water interface. The small symbols represent gas molecules in the air and dissolved in the water. The greater concentration of these symbols in the water on the left side of the diagram indicates that the dissolved gas is supersaturated in the water. The bubble-induced flux, F_B, into surface waters, illustrated on the right side of the diagram, is balanced by a diffusive flux across the air-water interface, F_{AWI}, indicated on the left side.

BUBBLE INJECTION EFFECTS

1. Less soluble gases become more enriched in bubbles

2. Diffusion coefficients are approximately double in bubbles

3. Bubbles are pushed to depths of 20 m (P_t ~ 3 atm)

4. Air Injection- the total dissolution of the air in a bubble due to hydrostatic pressure

Gas	N_2	O_2	Ar	CO_2	Ne	He	Kr
Δ% sat	+7.7	+3.8	+3.5	+0.1	+11.6	+13.8	+1.8

From the total dissolution of a bubble (1 cm^3) of air at STP (15°C and S =35) in 1 m^3

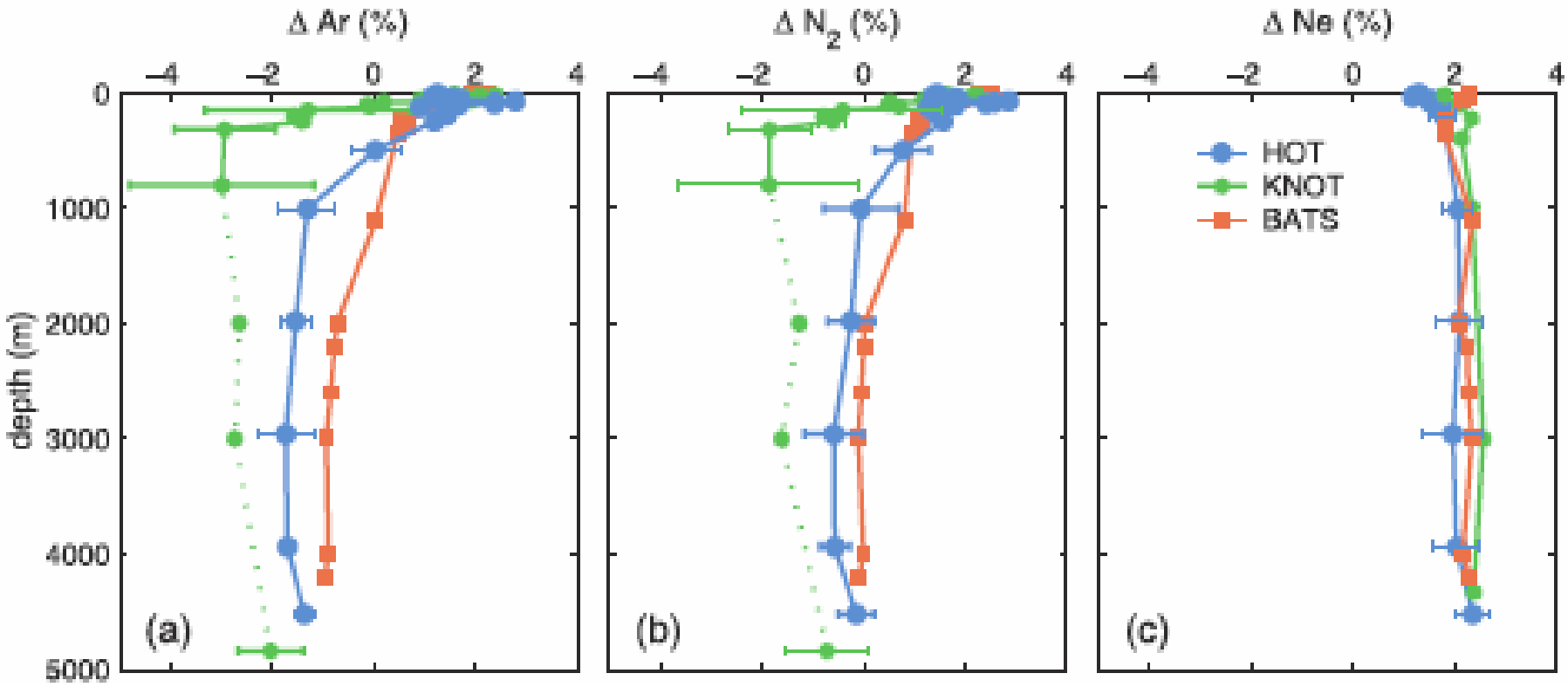
Δ Ar (%)
Δ N_2 (%)
Δ Ne (%)
−4
−2
0
2
4
0
1000
2000
3000
4000
5000
depth (m)
(a)
(b)
(c)
HOT
KNOT
BATS

Hamme & Emerson, 2002

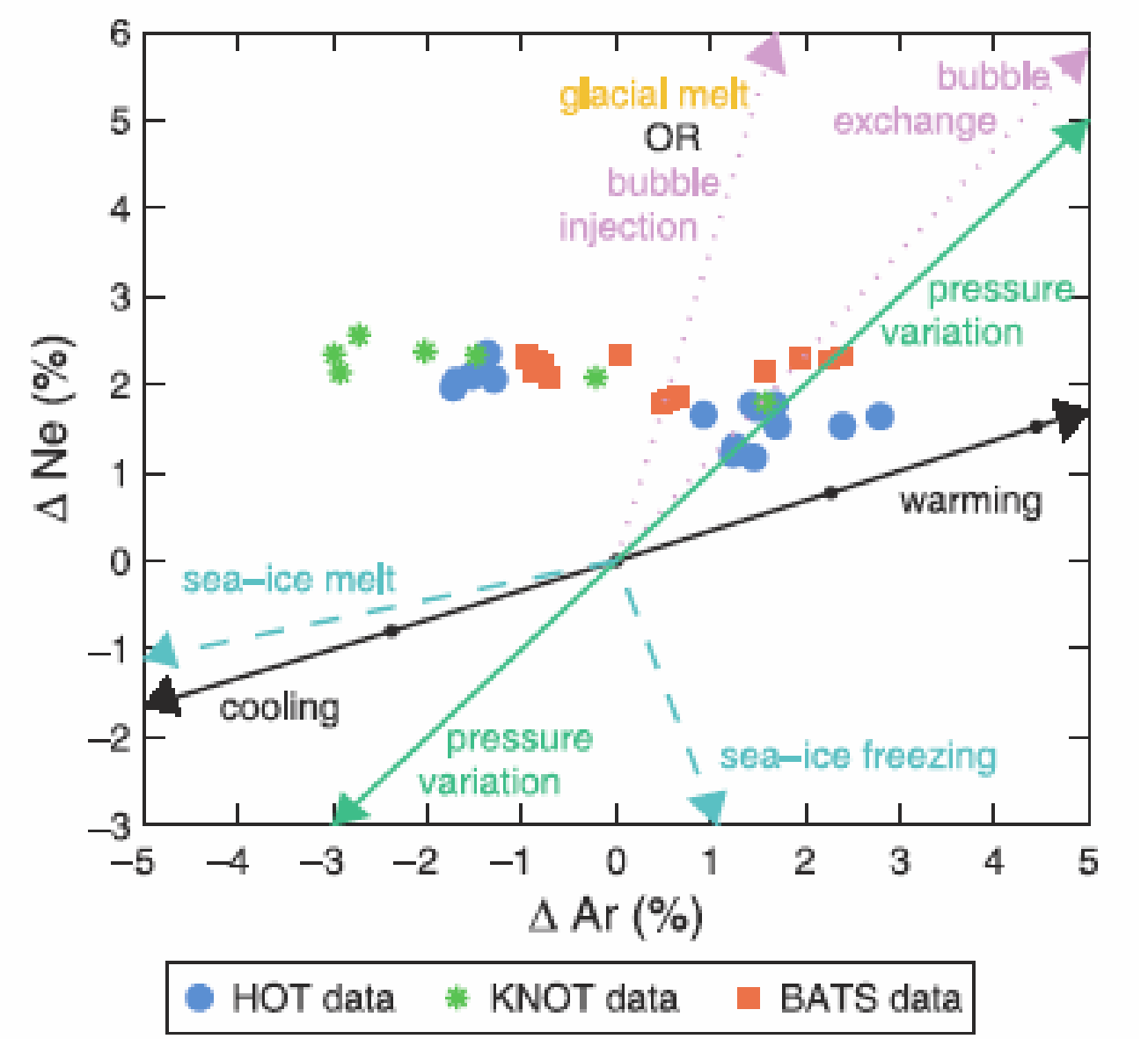

Dissolved Gases in Seawater

- Fundamentals
- Solubility Relationships
- Air-Sea Exchange
- Departures from Ideality
- O_2 Dynamics (Intro)

% O_2 sat = O_2 obs/O_2 sat x 100

AOU = O2 sat - O2 obs

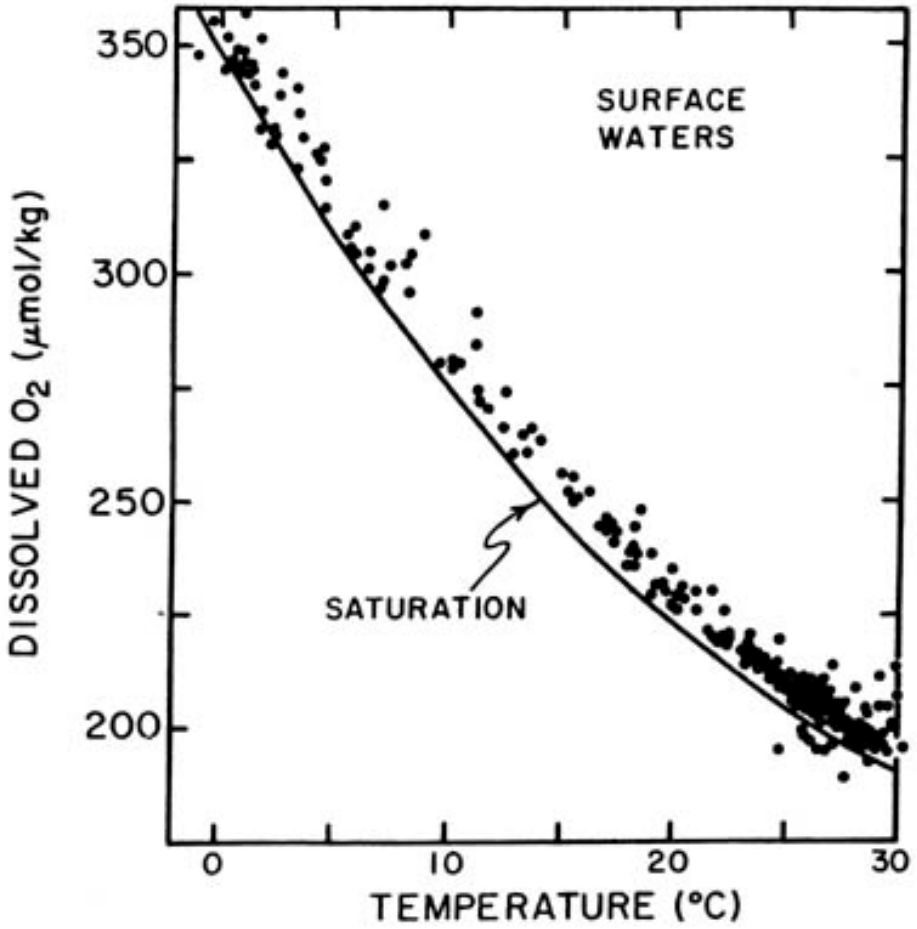

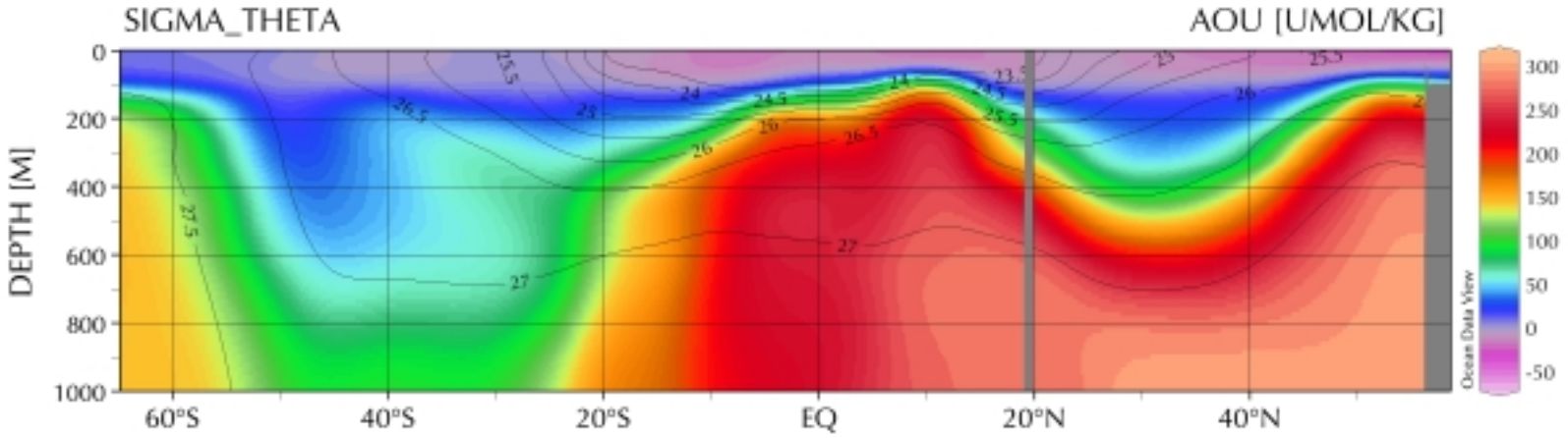
SIGMA_THETA
AOU [UMOL/KG]
DEPTH [M]
0
200
400
600
800
1000
60°S
40°S
20°S
EQ
20°N
40°N
300
250
200
150
100
50
0
-50
Ocean Data View

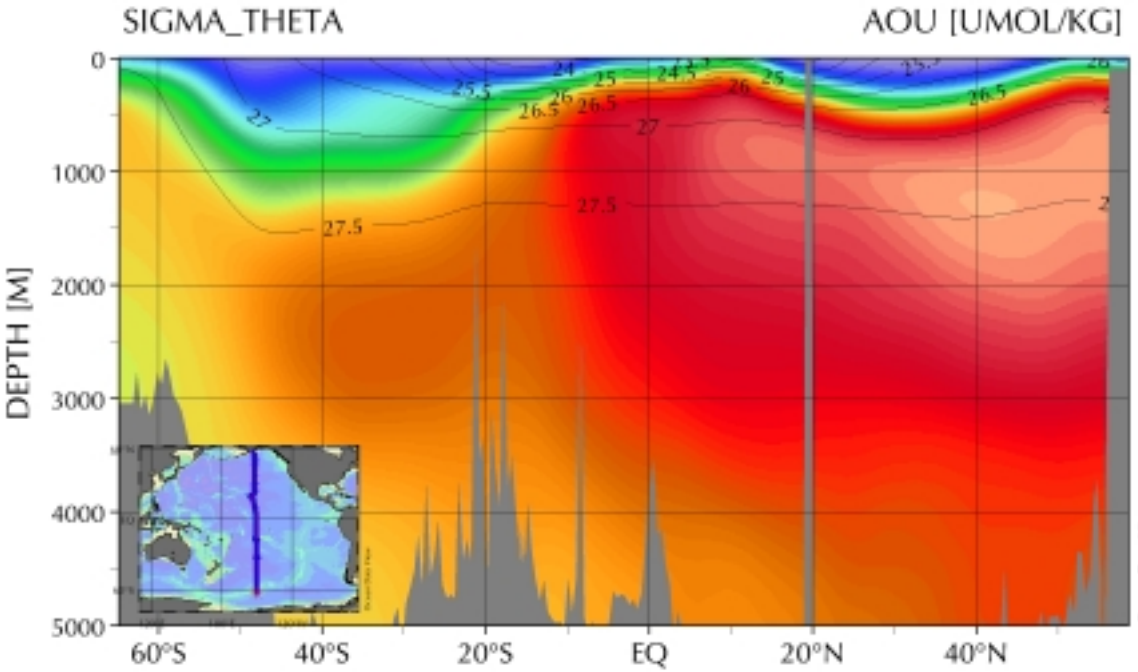
SIGMA_THETA
AOU [UMOL/KG]
DEPTH [M]
0
1000
2000
3000
4000
5000
60°S
40°S
20°S
EQ
20°N
40°N
300
250
200
150
100
50
0
-50
Ocean Data View

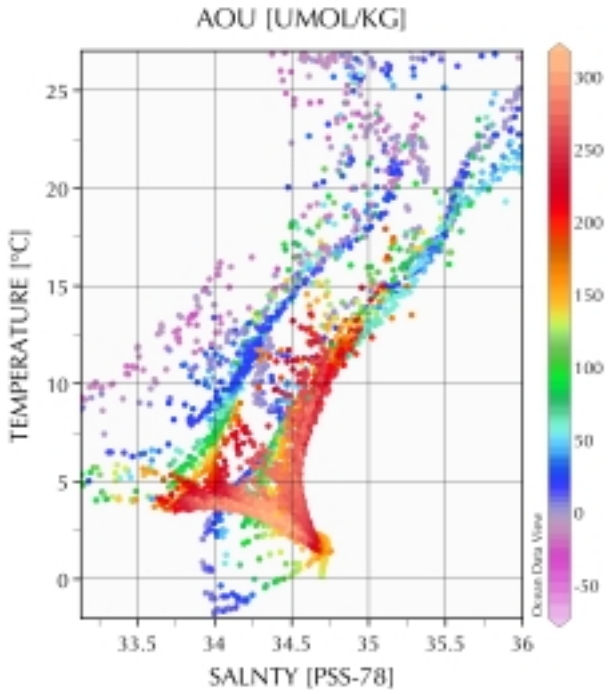
AOU [UMOL/KG]
TEMPERATURE [°C]
25
20
15
10
5
0
33.5
34
34.5
35
35.5
36
SALNTY [PSS-78]
300
250
200
150
100
50
0
-50
Ocean Data View

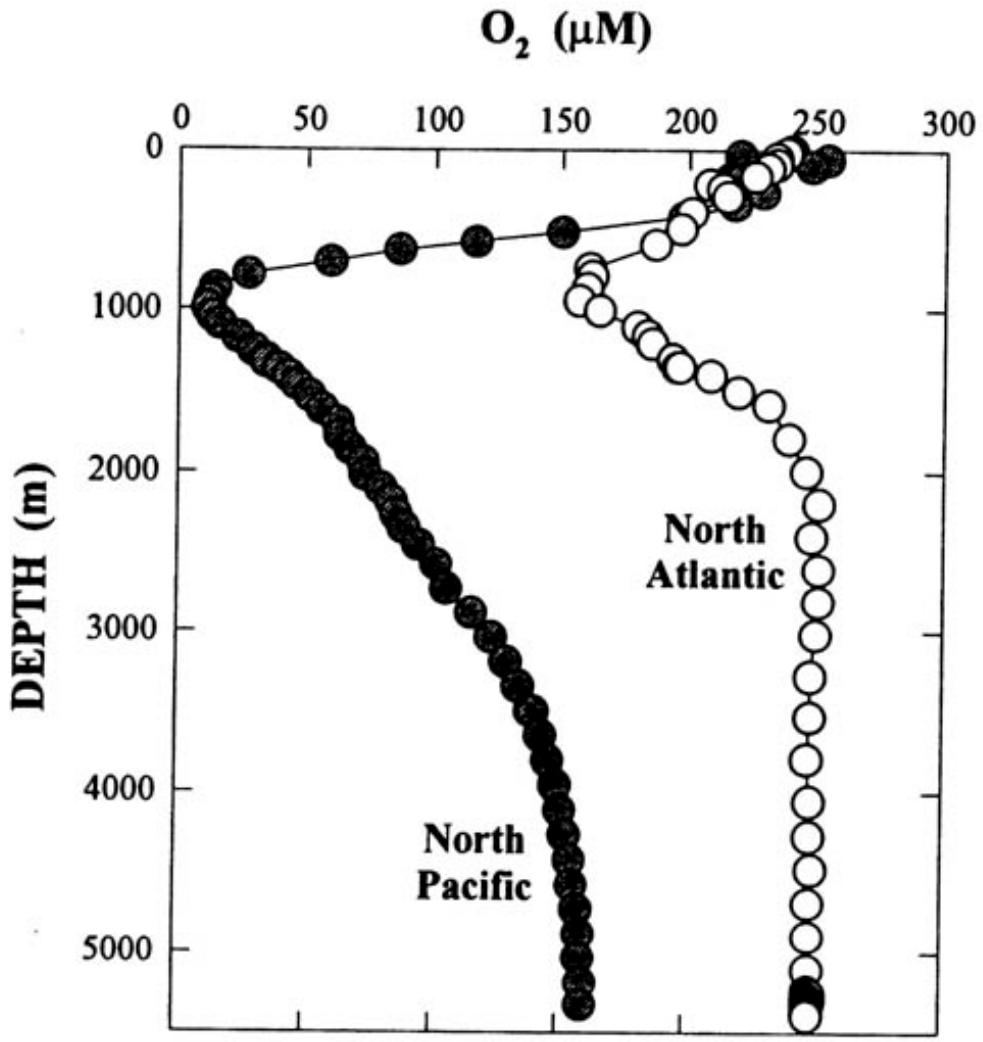

FIGURE 6.9. Profiles of oxygen in the North Atlantic and Pacific Oceans.

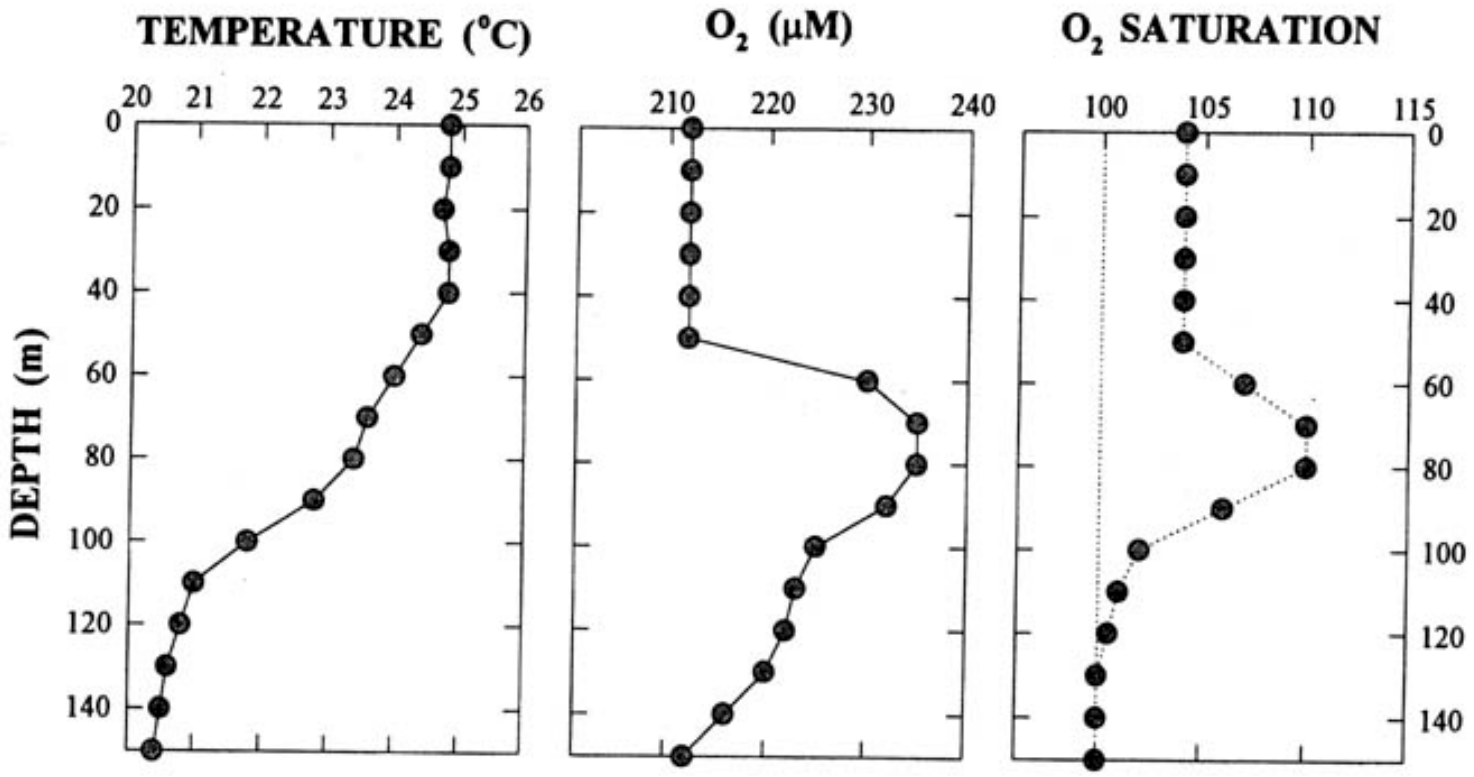

FIGURE 6.11. Profiles of temperature and oxygen in Pacific waters showing increases due to photosynthesis.

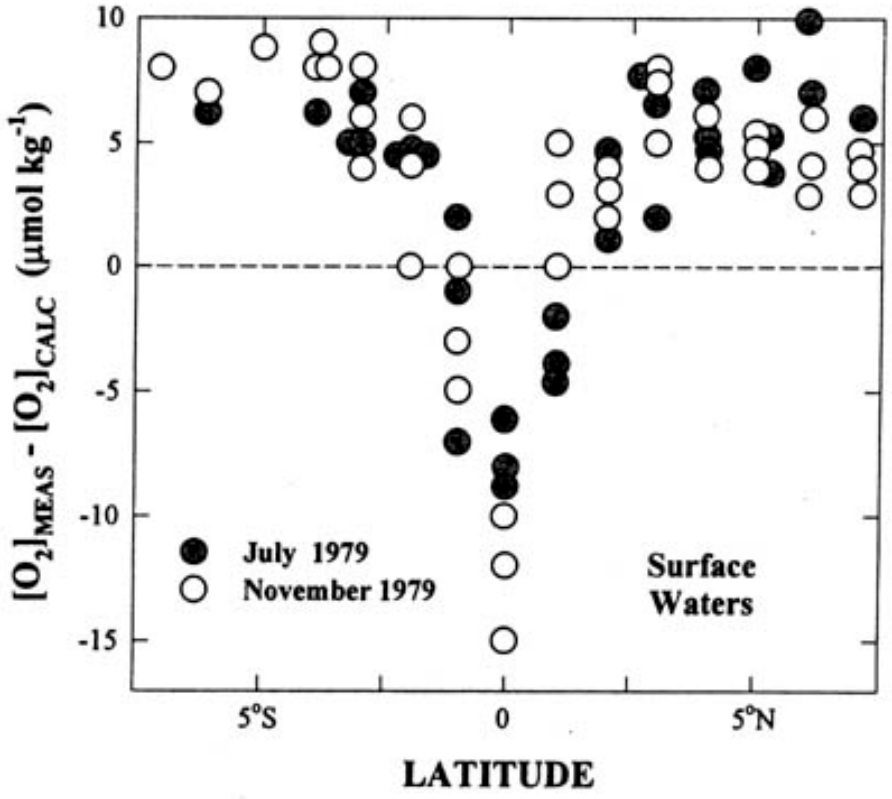

FIGURE 6.15. Differences in the measured and calculated dissolved oxygen concentrations in surface waters.

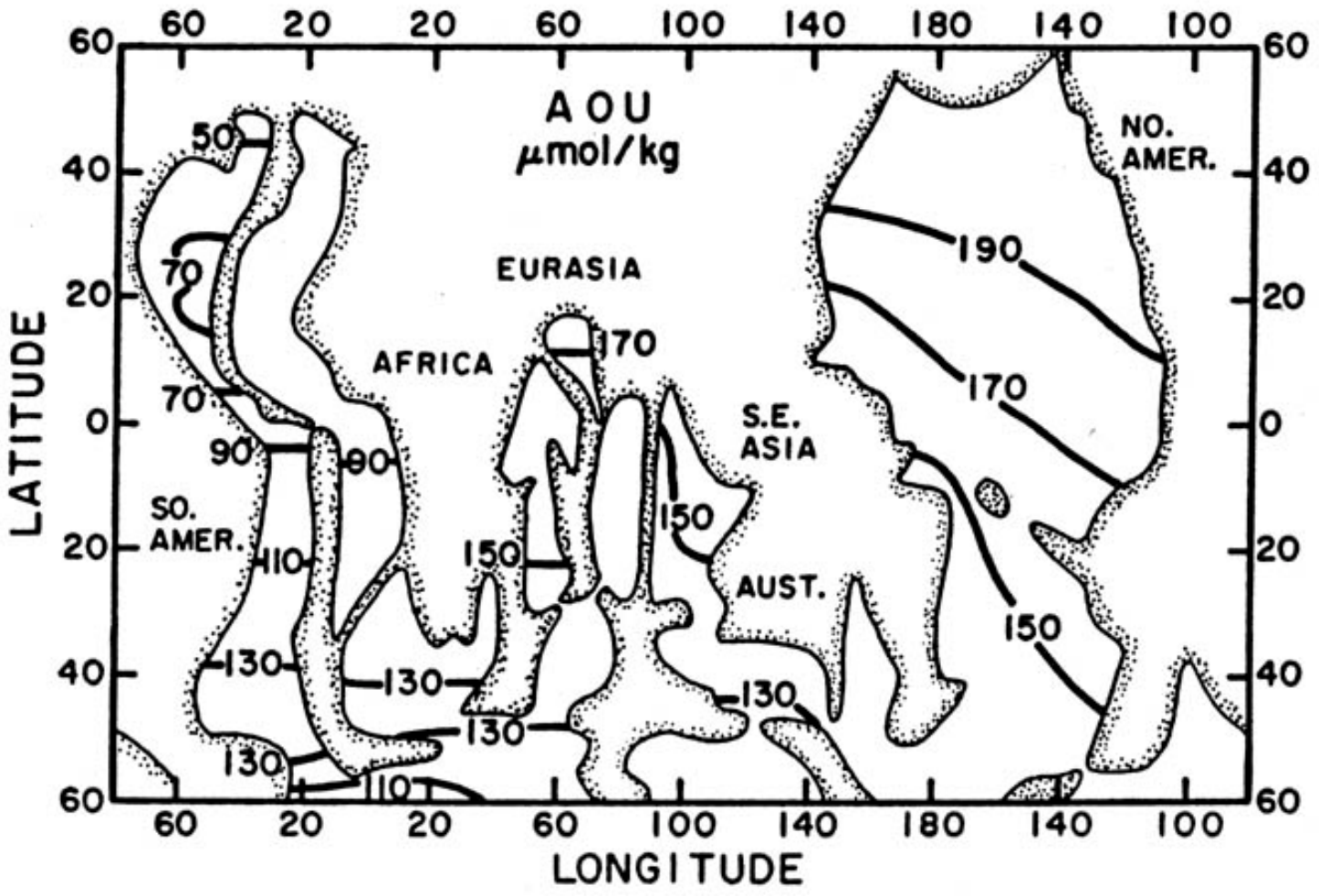

FIGURE 6.16. Apparent oxygen utilization in deep waters of the world oceans.

METHODS OF MEASUREMENT

1. Direct measurement in solution (O_2). Winkler Method for Oxygen

   A. $MnSO_4$ + NaOH Fixing Agent

   $Mn^{2+} + 2\ OH^- \rightarrow Mn(OH)_2$

   $2\ Mn(OH)_2 + O_2 \rightarrow 2\ MnO(OH)_2$

   B. Add KI, HCl and titrate with $S_2O_3^{2-}$

   $MnO(OH)_2 + 4H^+ + 2\ I^- \rightarrow$

   $Mn^{2+} + I_2 + 3H_2O$, $I_2 + I^- \rightarrow I_3^-$

   $I_3^- + 2\ S_2O_3^{2-} \rightarrow 3\ I^- + S_4O_6^{2-}$

2. Gas Chromatography (O_2,N_2,Ar,CO,CH_4)

3. Mass Spectrometry (low or non-reactive gases)